

Multicriticality and quantum fluctuation in generalized Dicke model

Youjiang Xu, Diego Fallas Padilla, Han Pu

We consider an important generalization of the Dicke model in which multi-level atoms, instead of two-level atoms as in conventional Dicke model, interact with a single photonic mode. We explore the phase diagram of a broad class of atom-photon coupling schemes and show that, under this generalization, the Dicke model can become multicritical. For a subclass of experimentally realizable schemes, multicritical conditions of arbitrary order can be expressed analytically in compact forms. We also calculate the atom-photon entanglement entropy for both critical and non-critical cases. We find that the order of the criticality strongly affects the critical entanglement entropy: higher order yields stronger entanglement. Our work provides deep insight into quantum phase transitions and multicriticality.

The Dicke model [1] is one of the most iconic models in quantum optics and quantum many-body physics. It describes an ensemble of two-level atoms interacting with a single photonic mode. When the atom-photon coupling strength exceeds a threshold, the system enters the superradiance phase via a second-order phase transition where the Z_2 symmetry of the model is spontaneously broken, and the photonic mode is macroscopically populated. The Dicke model and the superradiant quantum phase transition (SQPT) have been realized in various experimental settings, including quantum gases of neutral atoms [2–5], trapped ion system [6], super-conducting circuit [7–9], and solid state systems [10].

Real atoms, of course, possess complicated level structure. Even if we restrict ourselves to the ground state manifold, a typical atom often features more than two levels. This motivates our current work to investigate an important generalization of the Dicke model where the two-level atoms are replaced by multi-level atoms. As we shall show, this generalized Dicke model also supports the SQPT in the thermodynamic limit [11], but the order of the phase transition can now be controlled and multicritical points may emerge. We will provide a detailed study on the condition of the emergence of the multicritical points of arbitrary order, and show that higher order multicritical points are associated with a higher degree of atom-photon entanglement.

Our multicritical Dicke model describes N l -level atoms coupled with a single photonic mode of frequency ω . The Hamiltonian can be written as ($\hbar = 1$):

$$H = \omega a^\dagger a + \frac{g(a + a^\dagger)}{2\sqrt{N}} \sum_{k=1}^N d^{(k)} + \epsilon \sum_{k=1}^N h^{(k)}, \quad (1)$$

where a is the photon annihilation operator, dimensionless single-atom Hamiltonian h and dipole operator d act on the l inner states of atoms, g and ϵ set the energy scales of the atom-photon interaction and the internal energy of the atoms, respectively.

Multicritical points are special points on the critical manifold. Multicriticality is defined by deduction, i.e., an n^{th} -order critical manifold is the boundary of the $(n-1)^{\text{th}}$ -order critical manifold, and the ordinary critical points are defined to be 2nd order [12][13]. For ex-

ample, a tricritical point can appear where a discontinuous phase transition boundary and a 2nd-order critical line smoothly intersect [13–15]. Multicritical points often belong to a universality class different from that of the ordinary critical points [16, 17], so they may provide new insight into quantum phase transitions. Especially, because quantum criticality is characterized by increasing quantum fluctuation, we want to study how the quantum fluctuation is affected by multicriticality. However, systems that support high-order critical points are rarely found, for the reason that more than a few parameters need to be fine-tuned, and it is usually challenging to pinpoint the multicritical manifold in the phase space because the dimension of the manifold decreases when the order of criticality increases. Usually, the dimension of an n^{th} -order critical manifold is $(n-1)$ less than the number of tunable parameters [13]. It turns out that Hamiltonian (1) serves as a great platform to investigate multicriticality because: (1) It provides plenty of tunable parameters that are experimentally realistic; and (2) it is possible to derive exact analytical expressions of multicritical conditions, the equations that determines the multicritical manifolds.

We will first discuss the multicritical Dicke model within the mean-field framework. The mean-field Hamiltonian H_{MF} is obtained by replacing the bosonic operator a with a real number $\epsilon\sqrt{N}\phi/g$:

$$H_{\text{MF}}/\epsilon = \kappa\phi^2 + \phi d + h, \quad (2)$$

where $\kappa := \omega\epsilon/g^2$. We denote the eigenstates of H_{MF} as $|k\rangle$'s with eigenvalues ϵ_k ($k = 1, 2, \dots, l$). We assume that $|1\rangle$ is the non-degenerate ground state of H_{MF} . The mean-field ground state energy is obtained by minimizing ϵ_1 with respect to ϕ , and the ϕ that minimizes ϵ_1 is recognized as the order parameter. The SQPT occurs in the thermodynamic limit $N \rightarrow \infty$ when the order parameter becomes non-zero.

The Z_2 symmetry of Hamiltonian (1), which is spontaneously broken by the SQPT, manifests itself as H is invariant under the transformation $a \rightarrow -a$, $d \rightarrow -d$, $h \rightarrow h$. Given this symmetry, the mean-field ground state energy can be written as a Taylor series in terms of ϕ^2 : $\epsilon_1 = \sum_{k=0}^{\infty} c_k \phi^{2k}$. An ordinary critical point is met when $c_1 = 0$ and $c_2 > 0$. The boundary of this mani-

fold satisfies the condition $c_1 = c_2 = 0$, which specifies the tricritical manifold. Generally, the n^{th} -order critical manifold satisfies the condition $c_1 = c_2 = \dots = c_{n-1} = 0$. These multicritical conditions can be expressed as equations on d and h using perturbation theory. Treating h as the unperturbed Hamiltonian and ϕd as the perturbation, we obtain c_k by carrying out the perturbation expansion to $(2k)^{\text{th}}$ order. For example, the 2nd-order perturbation expansion recasts $c_1 = 0$ as

$$\sum_{k=2}^l \frac{|d_{1k}|^2}{h_{kk}} = \kappa, \quad (3)$$

where the matrix elements are taken respect to the eigenvectors of h that satisfies $h_{kk} > h_{11} = 0$ for $k = 2, 3, \dots, l$. The 4th-order perturbation recasts $c_2 = 0$ as:

$$\sum_{k_1 k_2 k_3=2}^l \frac{d_{1k_1} d_{k_1 k_2} d_{k_2 k_3} d_{k_3 1}}{h_{k_1 k_1} h_{k_2 k_2} h_{k_3 k_3}} = \sum_{k_1 k_2=2}^l \frac{|d_{1k_1}|^2 |d_{1k_2}|^2}{h_{k_1 k_1}^2 h_{k_2 k_2}}. \quad (4)$$

and so on so forth.

In general, the existence of the n^{th} -order critical points requires at least $(n-1)$ tunable parameters. For the multicritical Dicke model considered here, the number of internal atomic levels l and the Z_2 symmetry put constraints on the number of tunable parameters. The Z_2 symmetry requires the presence of a parity operator P which makes $PdP = -d$ and $PhP = h$. Suppose the number of ± 1 in the eigenvalues of P is $\frac{l \pm \delta}{2}$. If we represent d and h as matrices using a set of common eigenvectors of h and P as basis, then h is diagonal and contains l tunable parameters, which are just the eigenvalues of h ; whereas d must be in the form $d = \begin{pmatrix} 0 & M \\ M^\dagger & 0 \end{pmatrix}$

where M is an arbitrary $\frac{l-\delta}{2} \times \frac{l+\delta}{2}$ matrix. Now we have $\frac{l^2-\delta^2}{2} + l$ parameters, besides, we have to fix the $(l-1)$ relative phases between the common eigenvectors, also the physics would not change if we rescale H or shift the zero point energy. In the end, we have at most $G = (l^2 - \delta^2)/2 - 1$ tunable parameters. For example, for two-level atoms with $l = 2$ as in the conventional Dicke model, we have $\delta = 0$ and $G = 1$, which means no multicriticality. In order to find multicriticality, we must have at least $l = 3$. We note that a tricritical point is identified in a spin-1 Bose gas subjected to spin-orbit coupling [18]. This system can be recast into the form of the generalized Dicke model with $l = 3$ in the classical oscillator limit. In our previous work [19], by introducing a staggered magnetic field to the two-level atoms, we show that this modified Dicke model exhibits tricriticality. This model can be regarded as a special case of the generalized Dicke model with $l = 4$.

Although the procedure of finding the multicritical condition of any order is straightforward under the perturbation approach outlined above, Eqs. (3) and (4) indicate that these equations quickly become very complicated as the order increases. Even numerical solutions

to these equations may become impractical. However, we will show now that, for a subclass of the multicritical Dicke models, we can write down the multicritical conditions to arbitrary order in compact analytic forms. For this subclass, still under the representation where h is diagonal, only the super- and sub-diagonal elements of the d matrix are non-vanishing, i.e., $d_{ij} = 0$ if $|i-j| \neq 1$. As a result, H_{MF} takes a tridiagonal form, and hence we call this subclass as the T-class. For a T-class Hamiltonian, the n^{th} -order critical condition is given by the simple form

$$|d_{k,k-1}|^2 = \kappa h_{kk}, \quad \text{for } 2 \leq k \leq n. \quad (5)$$

To prove it, we denote, for a given l , the determinant of H_{MF} as ζ_l , which can be expressed as a Taylor series of ϕ^2 . If $c_1 = c_2 = \dots = c_{n-1} = 0$, then $\zeta_l \propto \phi^{2n}$. We shall now prove that $\zeta_l \propto \phi^{2n}$ as long as Eq. (5) holds. To this end, we write down the recurrence relation for ζ_k by exploiting the tridiagonal form of H_{MF} :

$$\zeta_k = (h_{kk} + \kappa \phi^2) \zeta_{k-1} - \phi^2 |d_{k,k-1}|^2 \zeta_{k-2}.$$

Under the condition of Eq. (5), we have $\zeta_2 = \kappa^2 \phi^4$, $\zeta_3 = \kappa^3 \phi^6$. By deduction, it is easy to prove $\zeta_k = \kappa^k \phi^{2k}$ for $k = 2, 3, \dots, n$. As a result, ζ_l must be proportional to ϕ^{2n} for $n \leq l$, which finishes the proof.

The experimental scheme for realizing a T-class Hamiltonian has been proposed in [20] and realized in [21]. Using the $F = 2$ hyperfine ground state of ^{85}Rb with cavity-assisted Raman transitions, it is possible to realize up to 5th-order criticality following the critical conditions Eq. (5). With one pair of Raman lasers as proposed in [20], the relative strength between $d_{n,n-1}$'s are fixed as $(d_{12}, d_{23}, d_{34}, d_{45}) = (\sqrt{2}, \sqrt{3}, \sqrt{3}, \sqrt{2})$, which will always be used in our numerical studies. With this d matrix, the multicritical conditions are met by tuning h_{kk} 's, which represent the bare energies of the atomic internal states and which can be tuned with external magnetic fields via the Zeeman shift or external microwave fields via the AC-Stark shift [22–28]. We set $\kappa = 1$ in our numerical calculation, then the 5th-order critical point is located at $(h_{22}, h_{33}, h_{44}, h_{55}) = (2, 3, 3, 2)$.

In Fig. 1, we plot the phase diagrams of the T-class Hamiltonians that are experimentally available. In Fig. 1(a)(b), we show the change of the order parameter with respect to h , which is tuned around a tetracritical (i.e., 4th-order) point. This is done by setting h_{55} to be very large, hence we have effectively a 4-level atomic system. The tetracritical point is located at $(h_{22}, h_{33}, h_{44}) = (2, 3, 3)$ and is marked by the white dot in the graphs. In Fig. 1(a), we fix $h_{44} = 3$ and vary h_{22} and h_{33} . The darker region represents the normal phase and the lighter region the superradiance region. The ordinary 2nd-order critical line is marked by the white dashed line which is a straight line with $h_{22} = 2$ and $h_{33} > 3$. The phase boundary to the left of the tetracritical point is of 1st-order. In Fig. 1(b), we fix $h_{33} = 3$ and vary h_{22} and h_{44} . Here the straight solid line with $h_{22} = 2$ and $h_{44} > 3$

is a tricritical line, which joins the 1st-order boundary at the tetracritical point. In Fig. 1(c), we show the boundary surface between the normal (above the surface) and the superradiant phase (below the surface) in the full three dimensional parameter space. This boundary surface contains two parts: a flat part at plane representing the 2nd-order critical manifold and a curved part representing the 1st-order surface. The tricritical line and the tetracritical point are marked by the white solid line and the white dot, respectively.

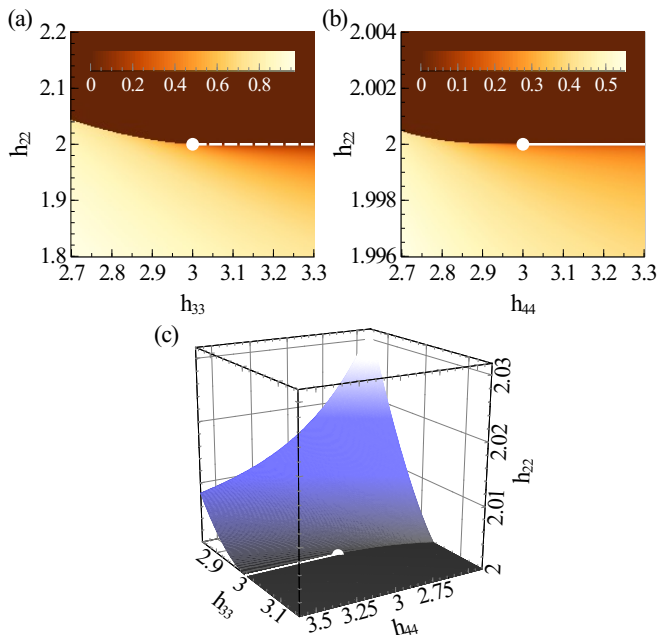


FIG. 1. (Color online) (a)(b) The mean-field phase diagram of a 4-level T-class Hamiltonian around the 4th-order critical point. The colorbar represents the order parameter ϕ . The dashed line in (a) is an ordinary critical line while the solid line in (b) is a tricritical line. (c) The boundary between the normal phase and the superradiant phase, in which h_{22} is plotted as a function of h_{33} and h_{44} . The $h_{22} = 2$ plane is the critical manifold, with a tricritical line marked by a solid line. The curved surface is the 1st-order phase transition boundary. In all panels, we use a white dot to mark the 4th-order critical point.

Having discussed the mean-field phase diagram, we now turn our attention to the quantum fluctuation and the entanglement properties of the model. By shifting the bosonic operator in Eq. (1) by the mean-field order parameter, $b := a - \epsilon\sqrt{N}\phi/g$, Eq. (1) is rewritten as

$$H = \omega b^\dagger b + \frac{g(b^\dagger + b)}{2\sqrt{N}} \sum_{k=1}^N D^{(k)} + \sum_{k=1}^N H_{\text{MF}}^{(k)}, \quad (6)$$

where the shifted dipole operator is $D := d + 2\kappa\phi$.

Without loss of generality, the atomic states can be expressed in terms of an orthonormal basis consisting of completely symmetrized Fock states $|\chi\rangle$, where χ is

a vector whose component χ_i denote the number of atoms occupying $|i\rangle$, the i^{th} eigenstate of H_{MF} . Consequently, the last term in Eq. (6) is diagonal in this basis, $\langle \chi | \sum_{k=1}^N H_{\text{MF}}^{(k)} | \chi \rangle = \sum_{i=1}^l \epsilon_i \chi_i$. The non-zero matrix elements of $\sum_{k=1}^N D^{(k)}$ under the basis $|\chi\rangle$'s are

$$\langle \chi | \sum_{k=1}^N D^{(k)} | \chi \rangle = \sum_{k=1}^N \chi_k D_{k,k}, \quad (7)$$

$$\langle \chi^{i,j} | \sum_{k=1}^N D^{(k)} | \chi \rangle = \sqrt{\chi_j (\chi_i + 1)} D_{i,j}, \quad (8)$$

where $|\chi^{i,j}\rangle$ is the very state containing one more atom in $|i\rangle$ and one less atom in $|j\rangle$ than $|\chi\rangle$. As long as we are interested in the low-energy states, we can assume that most atoms occupy the mean-field ground state $|1\rangle$, i.e., $\chi_1 \sim N$ and $\chi_k = o(N)$ for $k = 2, 3, \dots, l$. We can then express $H = H_{\text{eff}} + N\epsilon_1 + o(1)$ when $N \rightarrow \infty$, and the low-energy effective Hamiltonian H_{eff} is quadratic in b and new bosonic operators b_2, b_3, \dots, b_l :

$$H_{\text{eff}} = \omega b^\dagger b + \sum_{i=2}^l \left[\omega_i b_i^\dagger b_i + \frac{g}{2} |D_{1,i}| (b + b^\dagger) (b_i + b_i^\dagger) \right], \quad (9)$$

where b_i is defined by $b_i |\chi^{1,i}\rangle = \sqrt{\chi_i} |\chi\rangle$, and $\omega_i = \epsilon_i - \epsilon_1$. In deriving Eq. (9), we have used $D_{1,1} = 0$, which results from the steadiness of the mean-field energy $\partial_\phi \epsilon_1 = 0$. Because the leading term in the asymptotic series of H is the mean-field energy $N\epsilon_1$, it serves as a confirmation that the mean-field theory determines the exact phase diagram as long as the asymptotic expansion is valid. The validity of the expansion can be verified self-consistently, i.e., it is valid as long as $\sum_{i=2}^l \langle b_i^\dagger b_i \rangle \ll N$, where the expectation value is taken in respect to the low-energy states.

To find the ground state of H_{eff} , the effective Hamiltonian can be transformed into a Hamiltonian describing an l -dimensional harmonic oscillator,

$$H_{\text{eff}} = \frac{1}{2} \sum_{j,k=1}^l (P_j \delta_{jk} P_k + X_j \Omega_{jk}^2 X_k) - \frac{1}{2} \sum_{k=1}^l \omega_k, \quad (10)$$

where $P_k = \sqrt{\frac{\omega_k}{2}} (b_k - b_k^\dagger)$ and $X_k = \frac{1}{\sqrt{2\omega_k}} (b_k + b_k^\dagger)$ are canonical momentum and position operators as linear combinations of b_k and b_k^\dagger . Here we have denoted $b_1 \equiv b$ and $\omega_1 \equiv \omega$. The squared eigenfrequencies of the harmonic oscillator are given by the eigenvalues of the matrix Ω^2 . The non-zero matrix elements of Ω^2 are given by

$$\begin{aligned} \Omega_{kk}^2 &= \omega_k^2, \text{ for } k = 1, 2, \dots, l, \\ \Omega_{1k}^2 &= |D_{1,k}| \sqrt{\omega_k}, \text{ for } k > 1. \end{aligned}$$

The eigenvalues of Ω^2 are determined by the character-

istic polynomial

$$p(\lambda^2) = \left(1 - \sum_{k=2}^l \frac{|D_{1,k}|^2 \omega \omega_k}{(\omega^2 - \lambda^2)(\omega_k^2 - \lambda^2)}\right) \prod_{k=1}^l (\omega_k^2 - \lambda^2),$$

If $\omega_{j-1} \neq \omega_j = \omega_{j+1} = \dots = \omega_{j+f} < \omega_{j+f+1}$, then $\lambda^2 = \omega_j^2$ must be an f -fold eigenvalue. The corresponding eigenstates are trivial in the sense that they are dark states which do not couple to the light mode. In studying the SQPT, we are not interested in these dark states so we remove the degeneracy by requiring $\omega_j < \omega_{j+1}$ for $j > 1$. Now the characteristic equation is equivalent to

$$q(\lambda^2) := \omega^2 - \lambda^2 + \omega \sum_{k=2}^l \frac{|D_{1,k}|^2 \omega_k}{\lambda^2 - \omega_k^2} = 0,$$

from which we notice the distribution of the solutions: $\lambda_1^2 \in (-\infty, \min(\omega^2, \omega_2^2))$, $\lambda_2^2 \in (\omega_2^2, \omega_3^2)$, \dots , $\lambda_l^2 \in (\omega_l^2, +\infty)$. We note that only λ_1 can be zero as long as the mean-field ground state is non-degenerate. The asymptotic expansion is valid when $\lambda_1^2 > 0$, otherwise the fluctuation blows up. Consequently, the equation $q(0) = 0$ gives the critical condition, which coincides with the one derived through the mean-field theory in Eq. (3).

The ground state wave function of H_{eff} is an l -dimension Gaussian function, whose atom-photon entanglement entropy can be calculated straightforwardly:

$$S = \frac{\gamma}{e^\gamma - 1} - \ln(1 - e^{-\gamma}), \quad (11)$$

$$\gamma = \cosh^{-1} \left(\frac{\Omega_{11} M_{11} + \det \Omega}{\Omega_{11} M_{11} - \det \Omega} \right), \quad (12)$$

where M_{11} is the (1, 1)-minor of the matrix Ω . Here S is the von Neumann entropy of the reduced density matrix for either the atomic or the photonic modes. Because the critical condition can also be expressed as $\det \Omega = 0$ or $\gamma = 0$, the entropy diverges at the critical points. Near the critical points, γ is small, so approximately we have $S = 1 - \ln \gamma$, which indicates a logarithm divergence approaching the critical point. The entropy near the critical points is closely related to the fluctuation in the light mode, which can be read from the following equation

$$\langle (b^\dagger + b)^2 \rangle = \frac{\omega M_{11}}{\det \Omega}. \quad (13)$$

In addition, the entropy is closely related to the first excitation gap $\lambda_1 = \det \Omega / \prod_{i=2}^l \lambda_k$.

Finally, we examine the entanglement entropy at the critical points where the asymptotic expansion possibly fails. We numerically calculate the finite- N critical entropy for the T-class Hamiltonians. In the thermodynamic limit, the ground state is non-degenerate in the normal phase while doubly degenerate in the superradiant phase, and the excitation gap closes at the phase boundary and remains closed in the superradiance region. For finite N , however, the gap does not close, but

TABLE I. Asymptotic behavior of the critical entropy $S_{\text{cri}} \sim s_0 + s_1 \ln N$.

Order of Criticality	2	3	4	5
s_0	0.593(2)	0.642(7)	0.682(7)	0.704(8)
s_1	0.1428(7)	0.207(2)	0.238(3)	0.257(3)

rather decreases exponentially when we move deeper into the superradiant region. Therefore, the phase boundaries and the critical manifolds in a finite system cannot be determined unambiguously by the gap, as demonstrated in Fig. 2(b). Instead, we locate the critical manifold for finite N by maximizing the atom-photon entanglement entropy S by varying h_{22} , as shown in Fig. 2(c). The maximized entropy is identified as the critical entropy S_{cri} for finite N .

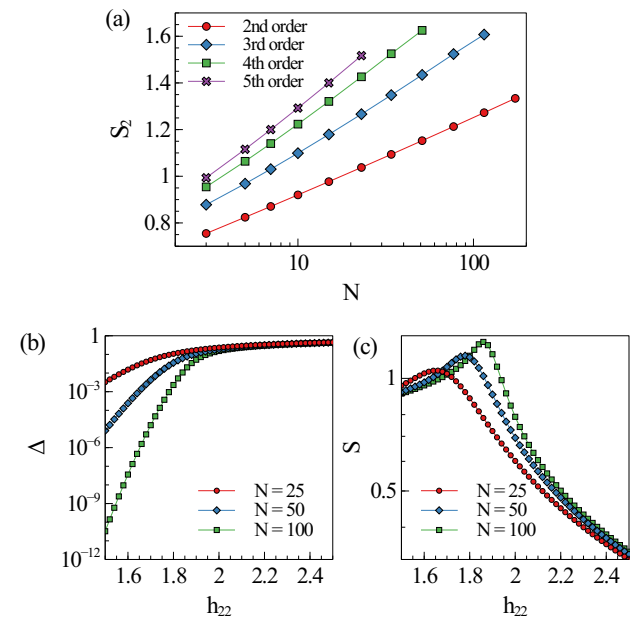


FIG. 2. (Color online) (a) Critical atom-photon entanglement entropy S_{cri} plotted against the atom number N for T-class Hamiltonians with different orders of criticality. (b) The gap Δ between the ground state and the first excited state, and (c) the ground state entropy S , of the two-level Dicke model with $d_{12} = \sqrt{2}$ for different atom number N . Δ exponentially decreases when h_{22} moves deep into the superradiant phase.

In Fig. 2(a), we plot S_{cri} against N at critical points with different order of criticality for the T-class Hamiltonians. Asymptotically, we have $S_{\text{cri}} \sim s_0 + s_1 \ln N$. The fitting parameters s_0 and s_1 are shown in Table I, from which we see that higher-order criticality is associated with a larger degree of entanglement. Different orders of criticality are achieved by setting $(h_{33}, h_{44}, h_{55}) = (3, 3, 2)$ then tuning some h_{kk} to infinity. For example, to achieve the tricriticality, we set $h_{44} = h_{55} = \infty$.

Conclusion — We replace the two-level atoms in conventional Dicke model with l -level atoms and study the

superradiance phase transition in the modified model. The increased number of tuning parameters for $l > 2$ leads to the emergence of multicriticality whose order can be controlled. The phase diagram and the multicritical conditions can be obtained from the mean-field theory. For subclass of the multicritical Dicke models, which can be readily realized experimentally, we show that the multicritical conditions of arbitrary order can be expressed analytically in compact forms. The non-critical atom-photon entanglement entropy of the multicritical Dicke models in the thermodynamic limit can be

calculated analytically through an asymptotic expansion of the Hamiltonian. The entropy diverges logarithmically when approaching the critical point. The entropy at the critical points for finite number of atoms are calculated numerically. We found that the critical entropy increases when the order of criticality increases. Our work provides deep insights into the physics of quantum phase transition and multicritical points, whose realization is typically very challenging in other contexts.

We acknowledge support from the NSF and the Welch Foundation (Grant No. C-1669).

-
- [1] R. H. Dicke, *Phys. Rev.* **93**, 99 (1954).
- [2] F. Dimer, B. Estienne, A. S. Parkins, and H. J. Carmichael, *Phys. Rev. A* **75**, 013804 (2007).
- [3] D. Nagy, G. Kónya, G. Szirmai, and P. Domokos, *Phys. Rev. Lett.* **104**, 130401 (2010).
- [4] K. Baumann, C. Guerlin, F. Brennecke, and T. Esslinger, *Nature* **464**, 1301 (2010).
- [5] Z. Zhang, C. H. Lee, R. Kumar, K. J. Arnold, S. J. Masson, A. L. Grimsmo, A. S. Parkins, and M. D. Barrett, *Phys. Rev. A* **97**, 043858 (2018).
- [6] A. Safavi-Naini, R. J. Lewis-Swan, J. G. Bohnet, M. Gärtner, K. A. Gilmore, J. E. Jordan, J. Cohn, J. K. Freericks, A. M. Rey, and J. J. Bollinger, *Phys. Rev. Lett.* **121**, 040503 (2018).
- [7] L. Lamata, *Sci. Rep.* **7**, 43768 (2017).
- [8] A. Mezzacapo, U. Las Heras, J. Pedernales, L. DiCarlo, E. Solano, and L. Lamata, *Sci. Rep.* **4**, 7482 (2014).
- [9] N. Langford, R. Sagastizabal, M. Kounalakis, C. Dickel, A. Bruno, F. Luthi, D. Thoen, A. Endo, and L. DiCarlo, *Nat. Commun.* **8**, 1715 (2017).
- [10] X. Li, M. Bamba, N. Yuan, Q. Zhang, Y. Zhao, M. Xiang, K. Xu, Z. Jin, W. Ren, G. Ma, S. Cao, D. Turchinovich, and J. Kono, *Science* **361**, 794 (2018).
- [11] SQPT is also present in the so-called classical oscillator limit, where the frequency of the bosonic mode tends to zero [29]. In the classical oscillator limit, the phase transition shares the same mean-field description as that in the thermodynamic limit, but the underlying quantum fluctuation is different. We will discuss the classical oscillator limit of the generalized Dicke model in a separate paper.
- [12] Exactly speaking, an n^{th} -order critical manifold is the intersection of multiple $(n - 1)^{\text{th}}$ -order critical manifolds, some of which, though, may not show up in the physically accessible phase space, e.g., excluded by the Z_2 symmetry in the model we study.
- [13] T. S. Chang, A. Hankey, and H. E. Stanley, *Phys. Rev. B* **8**, 346 (1973).
- [14] R. B. Griffiths, *Phys. Rev. Lett.* **24**, 715 (1970).
- [15] P. M. Chaikin, T. C. Lubensky, and T. A. Witten, *Principles of condensed matter physics*, Vol. 10 (Cambridge university press Cambridge, 1995).
- [16] E. K. Riedel, *Phys. Rev. Lett.* **28**, 675 (1972).
- [17] M. Henkel, *Conformal Invariance and Critical Phenomena* (Springer-Verlag Berlin Heidelberg, 2013).
- [18] D. Campbell, R. Price, A. Putra, A. Valdés-Curiel, D. Trypogeorgos, and I. Spielman, *Nat. Commun.* **7**, 10897 (2016).
- [19] Y. Xu and H. Pu, *Phys. Rev. Lett.* **122**, 193201 (2019).
- [20] S. J. Masson, M. D. Barrett, and S. Parkins, *Phys. Rev. Lett.* **119**, 213601 (2017).
- [21] Z. Zhiqiang, C. H. Lee, R. Kumar, K. J. Arnold, S. J. Masson, A. S. Parkins, and M. D. Barrett, *Optica* **4**, 424 (2017).
- [22] F. Gerbier, A. Widera, S. Fölling, O. Mandel, and I. Bloch, *Phys. Rev. A* **73**, 041602 (2006).
- [23] S. R. Leslie, J. Guzman, M. Vengalattore, J. D. Sau, M. L. Cohen, and D. M. Stamper-Kurn, *Phys. Rev. A* **79**, 043631 (2009).
- [24] E. M. Bookjans, A. Vinit, and C. Raman, *Phys. Rev. Lett.* **107**, 195306 (2011).
- [25] C. Cohen-Tannoudji and J. Dupont-Roc, *Phys. Rev. A* **5**, 968 (1972).
- [26] L. Santos, M. Fattori, J. Stuhler, and T. Pfau, *Phys. Rev. A* **75**, 053606 (2007).
- [27] K. Jensen, V. M. Acosta, J. M. Higbie, M. P. Ledbetter, S. M. Rochester, and D. Budker, *Phys. Rev. A* **79**, 023406 (2009).
- [28] A. de Paz, A. Sharma, A. Chotia, E. Maréchal, J. H. Huckans, P. Pedri, L. Santos, O. Gorceix, L. Vernac, and B. Laburthe-Tolra, *Phys. Rev. Lett.* **111**, 185305 (2013).
- [29] L. Bakemeier, A. Alvermann, and H. Fehske, *Phys. Rev. A* **85**, 043821 (2012).